

VideoDPO: Omni-Preference Alignment for Video Diffusion Generation

Runtao Liu^{1*} Haoyu Wu^{2*} Ziqiang Zheng¹ Chen Wei³
Yingqing He¹ Renjie Pi¹ Qifeng Chen¹
¹HKUST ²Renmin University of China ³Johns Hopkins University
rliuay@connect.ust.hk haoyuwu556@ruc.edu.cn

Abstract

Recent progress in generative diffusion models has greatly advanced text-to-video generation. While text-to-video models trained on large-scale, diverse datasets can produce varied outputs, these generations often deviate from user preferences, highlighting the need for preference alignment on pre-trained models. Although Direct Preference Optimization (DPO) [39] has demonstrated significant improvements in language and image generation [48], we pioneer its adaptation to video diffusion models and propose a VideoDPO pipeline by making several key adjustments. Unlike previous image alignment methods that focus solely on either (i) visual quality or (ii) semantic alignment between text and videos, we comprehensively consider both dimensions and construct a preference score accordingly, which we term the *OmniScore*. We design a pipeline to automatically collect preference pair data based on the proposed *OmniScore* and discover that re-weighting these pairs based on the score significantly impacts overall preference alignment. Our experiments demonstrate substantial improvements in both visual quality and semantic alignment, ensuring that no preference aspect is neglected. Code and data are available at <https://videodpo.github.io/>.

1. Introduction

With the rapid advancement of computing power and the increasing scale of training data, generative diffusion models have made remarkable progress in generation quality and diversity for video generation. However, current video diffusion models often fall short of meeting user preferences in both generation quality and text-video semantic alignment, ultimately compromising user satisfaction.

These issues often arise from the pre-training data, and filtering out all low-quality data is challenging given the vast often of pre-training data. Specifically, two types of

low-quality data are prevalent. First, regarding the videos themselves, some samples suffer from low resolution, blurriness, and temporal inconsistencies, which negatively impact the visual quality of generated videos. Second, regarding text-video pairs, mismatches between text descriptions and video content reduce the model’s ability to be controlled accurately through text prompts. Similar challenges are also seen in content generation for other modalities, such as language and image generation, where noisy pre-training data lowers output quality and reliability.

User preference alignment through Direct Preference Optimization, or DPO [39], has been proposed and tackles these issues well for language and image generation [48]. In this paper, we focus on aligning video diffusion models with user preferences with the idea of DPO with crucial adaption modifications, termed VideoDPO, described next.

First, we introduce a comprehensive preference scoring system, *OmniScore*, which assesses both the visual quality and semantic alignment of generated videos. We build the DPO reward model based on *OmniScore*. While existing visual reward models [23] typically focus on only one of these aspects, our experiments (see Fig. 3d) show that visual quality and semantic alignment, as well as various facets of visual quality, have low correlation. Addressing a single aspect does not inherently capture the others. Thus, a comprehensive scoring system like *OmniScore*, which integrates both dimensions, is crucial for accurate evaluation and alignment.

Second, obtaining preference annotations for generated videos is challenging due to the high cost of human labeling. To address this, we propose a pipeline that automatically generates preference pair data by strategically sampling from multiple videos conditioned on a given prompt, thereby eliminating the reliance on human annotation.

Third, to further improve the performance and efficiency of alignment training, we introduce a novel data re-weighting method, *OmniScore-Based Re-Weighting*. This approach is based on the intuition that certain preference pairs, particularly those with larger quality differences, have a greater impact on alignment. By analyzing the frequency

* Equal Contribution.



Figure 1. **Alignment results of VideoDPO from two different text-to-video models**, including VideoCrafter2 [7] (*first row*), and T2V-Turbo [26] (*second row*). More visualization results can be found in the supplementary materials.

distribution, we assign higher weights to these influential samples, prioritizing them during training. Experimental results show that our method delivers significant performance improvements while producing videos with high visual fidelity and precise semantic alignment, as shown in Fig. 1.

In summary, our contributions are:

(i) We pioneer the adaptation of DPO to video diffusion models, addressing the unique challenges of aligning video generation outputs with user preferences.

(ii) We introduce key adjustments to the DPO framework, including the development of OmniScore, a comprehensive preference scoring system, along with an automated preference data generation pipeline and a novel re-weighting strategy to enhance alignment training efficiency.

(iii) We validate our framework through extensive experiments conducted on three state-of-the-art open-source text-to-video models, evaluating performance across multiple metrics. The results demonstrate the robustness and effectiveness of our approach in improving both visual quality and semantic alignment.

2. Related Work

2.1. Text-to-Video Diffusion Models

The Text-to-Video (T2V) task aims to produce visually appealing videos that align with text input, ultimately striving to meet user requirements. It has wide applications across various domains, including story animation [15], controllable video generation [34, 35], video game development [5], and embodied artificial intelligence [9]. The predominant approaches for video generation [1, 2, 14, 49] employ diffusion-based models [18, 44]. Non-diffusion frameworks [10, 52, 54] have also shown significant progress. For instance, VideoCrafter [6, 7] utilizes a 1.4 billion parameter U-Net architecture for video generation, while models [19, 58, 63] such as Open-Sora [63] and CogVideoX [19, 58] are based on a Diffusion Transformer (DiT) backbone [8, 36].

Given the complexity of video data, transferring dif-

fusion pipelines to generate high-quality video content is a non-trivial task. This challenge is compounded by the necessity of implementing a series of post-training methods aimed at enhancing video quality. Existing methods include parameter efficient tuning [12, 16, 26, 27], data-centric work [13], and human preference alignment [37, 60] work. Despite the continuous expansion of training datasets and computational resources, the resulting video quality often falls short of user expectations.

2.2. RLHF and RLAI

Reinforcement Learning from Human Feedback (RLHF) is one of the most widely used post-training methods on large language models [57, 59, 62] and diffusion models. RLHF contains a reward model in the training stage and reinforcement learning stage. The reward model is trained on win-lose pairs annotated by humans by predicting the preference label. Prior works use policy-gradient [43] methods to align the policy model. The two-stage training pipeline is unstable and complex.

Preference alignment in diffusion models. DPO [39] is a reward model free method that can be easily performed on diffusion models. Despite the DPO-based methods being tested on text-to-image diffusion [48] models and gaining significant process, it has been rarely tested on T2V diffusion models. VADER [37] applies a reward model to refine a video diffusion model. T2V-turbo [26, 27] exploring training consistent distillation models by reward gradients. SPO [29] tries to improve quality on each step of the diffusion inverse process. T2V-turbo v2 [27] also uses a reward model for refinement. To the best of our knowledge, we are the first to propose to apply DPO-based method on video diffusion.

Visual content quality assessment. Previous video generation models often use metrics of Inception Score (IS) [41], Fréchet inception distance (FID) [17], Fréchet Video Distance (FVD) [47], and CLIPSIM [38] for evaluation. For text-to-image (T2I) models, several benchmarks [20, 25,

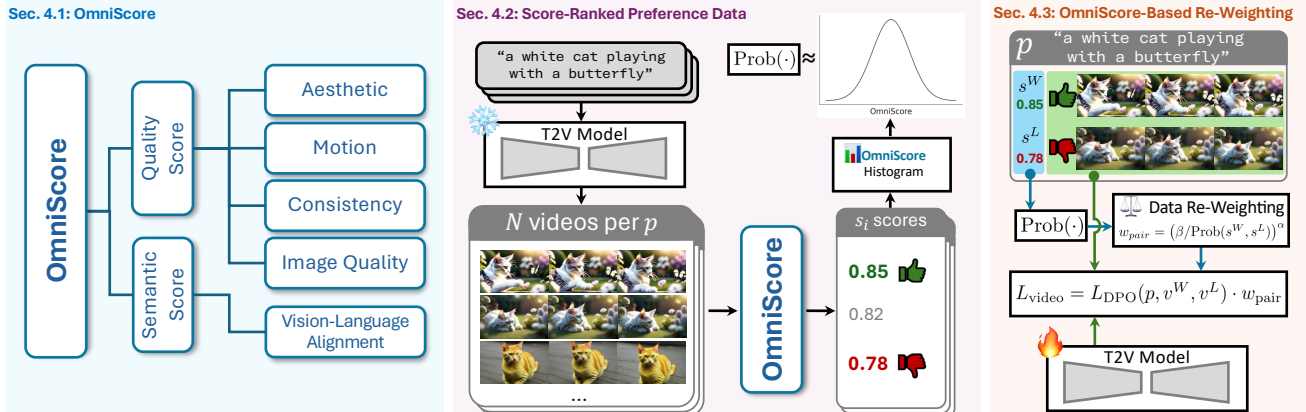


Figure 2. **VideoDPO pipeline.** We propose OmniScore to rate video sample quality with multi-dimensional scores (*left*). For each prompt, we generate N videos for each prompt p and score them using OmniScore. The highest and lowest scores, s^W and s^L for the corresponding videos v^W and v^L , form a preference pair to build the preference dataset. Additionally, we compute the frequency histogram of all videos’ OmniScore (*middle*). During training, preference pairs are re-weighted based on the frequency histogram. Typically, distinctive pairs which generally have lower sampling probabilities are assigned higher weights to help the model focus more on learning from them. (*right*).

40, 50]. Several benchmarks [21, 32, 33, 55] have been proposed to comprehensively evaluate the capabilities of video generation models. These benchmarks typically assess generation quality by using pre-trained score models [22, 38, 42, 46] to evaluate videos generated from a curated set of human-designed prompts. Other benchmarks, such as those for compositional video generation [45], story generation [3], chronological generation [61], and dynamic and motion quality [30, 31], focus on evaluating specific sub-tasks within video generation.

3. Preliminaries

3.1. Diffusion Models

For diffusion models, visual contents are generated by transforming a initial noise to the desired sample through multiple sequential steps. It is a Markov chain process where the model continually denoises the initial noise vector \mathbf{x}_T and finally generates a sample \mathbf{x}_0 .

The generation step from \mathbf{x}_t to \mathbf{x}_{t-1} is given by

$$\mathbf{x}_t \sim q(\mathbf{x}_t | \mathbf{x}_{t-1}) = \mathcal{N}(\mathbf{x}_t; \sqrt{\alpha_t} \mathbf{x}_{t-1}, \beta_t \mathbf{I}),$$

where β_t is the variance schedule, determining the amount of noise added at each timestep t . α_t is a parameter obtained by $\alpha_t = 1 - \beta_t$ which represents the proportion of the original data retained.

The denoising model ϵ_θ , which learns to predict the noise added to \mathbf{x}_0 for timestep t , is trained by minimizing the loss between the ground-truth ϵ and prediction. The loss function is defined as

$$L_d(\theta) = \mathbb{E}_{t, \mathbf{x}_0, \epsilon} \left[\|\epsilon - \epsilon_\theta(\sqrt{\alpha_t} \mathbf{x}_0 + \sqrt{1 - \alpha_t} \epsilon, t)\|^2 \right],$$

where ϵ is the noise added in the forward process, and $\bar{\alpha}_t$ is the cumulative product of α_t up to timestep t .

3.2. Direct Preference Optimization

DPO [39] is a technique used to align generative models with human preferences. Training on pairs of generated samples with positive and negative labels, the model learns to generate positive samples with higher probability and negative samples with lower probability. DiffusionDPO [48] adapts DPO for text-to-image diffusion models. The loss function provided in the [48] is defined as:

$$L_{\text{DPO}}(x^W, x^L, c) = L(x^W, p) - L(x^L, p),$$

where x^W and x^L represent positive and negative samples, respectively. $L(x^W, p)$ and $L(x^L, p)$ are losses for positive and negative parts, encouraging the model to generate samples closer to preferences.

4. VideoDPO

4.1. OmniScore

The quality of generated videos is influenced by multiple factors, which can be grouped into two main categories: visual quality and semantic alignment. Visual quality includes the clarity and richness of detail within each frame, *i.e.*, intra-frame quality, and the smoothness and coherence between frames, *i.e.*, inter-frame motion and consistency. Semantic alignment, on the other hand, focuses on whether the generated video accurately follows the text prompt. Inspired by VBench [21], we propose a scoring approach for video generation, OmniScore, which comprehensively accounts for both visual quality and semantic alignment of generated videos. OmniScore incorporates both quality and semantic sub-scores, specifically designed to evaluate video generation on three primary dimensions: the fidelity and aesthetics of visual quality, the smoothness of inter-frame transitions, and the level of semantic alignment

with the text. Each model for these dimensions is provided in the Appendix. This holistic approach enables a balanced method for preference pair data generation.

Intra-frame quality. Intra-frame quality includes two main metrics, image quality and aesthetic appeal. These metrics assess the visual quality of individual frames measuring image fidelity and aesthetic attractiveness. They provide a thorough evaluation of the frame-level visual detail, ensuring each frame is not only of high-fidelity but also visually engaging.

Inter-frame quality. Inter-frame quality focuses on the relationships between consecutive frames, examining how well they connect over time. This dimension includes metrics for subject consistency and background consistency, which assesses the stability of key elements across frames, ensuring that the main subject and background remain visually coherent. Additionally, it evaluates motion dynamics through three metrics: temporal flickering, motion smoothness, and the degree of motion dynamics. These collectively examine the video’s fluidity, ensuring smooth transitions between frames, minimizing visual disruptions, and maintaining a natural level of movement. By considering these aspects, we aim to ensure that the video maintains visual continuity and avoids disruptions that can detract from the viewing experience.

Text-video semantic alignment. Semantic alignment evaluates how closely the video content aligns with the text prompt. Using a foundational vision-language model, this score measures how accurately the video reflects the text and captures the user’s intent.

4.2. Score-Ranked Preference Data Generation

To construct the dataset of preference pairs, the scoring method, OmniScore, is employed in combination with a best vs. worst selection strategy. For each prompt, our system generates multiple videos and a preference pair is selected. Specifically, the video with the highest OmniScore is identified as the preferred video v^W , while the video with the lowest score is designated as the negative one v^L , as shown in Fig. 2. We utilize VidProm [51], a dataset of human-written text-to-video prompts, in our data construction process, enabling the model to better adapt to the distribution of real-world human inputs.

Video generation and scoring. Given a text prompt p , we generate a set of N videos $\{v_1, v_2, \dots, v_N\}$, using the pre-trained video generation model that we aim to align. For each generated video v_i , we apply the OmniScore model S to evaluate its quality conditioned on the text prompt p . This scoring model assigns a score to each video:

$$s_i = S(v_i, p), \text{ for } i = 1, 2, \dots, N. \quad (1)$$

Here, s_i denotes the OmniScore assigned to video v_i given its prompt p . This scoring step creates a quantitative basis for comparing videos generated from the same prompt.

Preference pair selection. We select preference pairs (v_i, v_j) from the N generated videos according to their OmniScore $\{s_1, s_2, \dots, s_N\}$. We select the video with the highest score as the winning sample v^W and the video with the lowest score as the negative sample v^L . This selection process is formalized as follows:

$$(v^W, v^L) = (v_i, v_j), i = \arg \max_i s_i, j = \arg \min_j s_j. \quad (2)$$

By constructing preference pairs consistently with maximum contrasting scores, we aim to establish clear distinctions between the preferred, or winning, and the less-preferred, or losing video samples. This strategy serves as a strong foundation for training the alignment model. We discuss several other selection strategies in Sec. 5.4.

4.3. OmniScore-Based Data Re-Weighting

Previous DPO training directly uses winning and losing preference pairs, for example, those generated as described in Sec. 4.2. However, we find the score difference between some winning and negative samples can be minimal, or in some cases, nearly identical, making it challenging for the model to effectively distinguish these samples with minor differences. To address this, we propose assigning higher weights to preference pairs with clearer distinctions, enabling the model to focus on those pairs that could provide more meaningful alignment cues. Our approach significantly enhances the model’s ability to learn meaningful alignment preferences.

Specifically, we first construct a histogram of OmniScore s of each generated video, including $K \times N$ videos from K prompts in total. We denote $p(\cdot)$ as the frequency and we define a function $p(\cdot)$ to approximate the probability of a video based on its frequency within these bins.

For each winning-losing pair, we define the pair probability as the geometric mean of their individual probabilities, i.e., $\text{prob}(s^W, s^L) = \sqrt{p(s^W) \cdot p(s^L)}$, where s^W and s^L represent the scores of the winning (positive) and losing (negative) samples, respectively. We define the re-weighting factor for each pair as:

$$w_{\text{pair}} = (\beta / \text{prob}(s^W, s^L))^\alpha. \quad (3)$$

Here, β is a constant set to the approximate probability of the most frequent sample, and α is a tuning hyperparameter. When α equals to 0, no re-weighting is applied, and all pairs have equal weight. A larger α increases the weight for pairs with lower probability.

The final training loss for each video pair is defined as:

$$L_{\text{video}} = L_{\text{DPO}}(p, v^W, v^L) \cdot w_{\text{pair}}, \quad (4)$$

where L_{DPO} refers to the DPO loss described in Sec. 3.2. The re-weighting factor w_{pair} adjusts the impact of each pair, encouraging the model to learn more effectively from those with clearer distinctions.

5. Experiment

5.1. Experiment Setup

Baselines. We compare our pipeline with several state-of-the-art open-source models for text-to-video generation: VideoCrafter-v2(VC2) [7], T2V-Turbo(Turbo) [26], and CogVideo [19]. These models are utilized as baselines in our alignment experiments. Additionally, we include VADER[37], which directly fine-tunes video diffusion models in several final steps using the differentiable reward model. We compare our method with their publicly released weights.

Metrics. To evaluate our method and the baselines, we use the following metrics: VBench, a widely recognized benchmark that assesses both quality and semantic alignment in video generation across 16 hierarchical dimensions, providing fine-grained evaluation. HPS (V) [56] and PickScore [23] are also included as metrics; both are trained on large-scale human preference datasets and are designed to predict scores of human preference for generated videos.

Implementation details. We train the video diffusion models for 3000 steps with a global batch size of 8, using the AdamW optimizer with a learning rate of $6e-6$. During training, the re-weighting algorithm hyper-parameters are set to $\alpha = 0.72$ and $\beta = 1$. $K = 10,000$ human-written prompts from VidProm [51] are used for alignment training. For each prompt, the number of generated videos N is set to 4. The bin width for the distribution of video OmniScore scores is set to 0.01. All experiments are conducted on 4 Nvidia A100 GPUs.

Model	VBench (%)			HPS (V)	PickScore	
	Total	Quality	Semantics			
VC2	Baseline[7]	80.44	82.20	73.42	0.258	20.65
	SFT	78.78	79.90	74.32	0.258	20.35
	VADAR[37]	80.59	82.46	73.09	0.259	20.62
	VideoDPO	81.93	83.07	77.38	0.261	20.65
Turbo	Baseline[26]	80.95	82.71	73.93	0.262	21.15
	VideoDPO	81.80	83.80	73.81	0.260	21.18
CogVid.	Baseline [19]	79.30	82.35	67.10	-	19.81
	SFT	79.64	82.74	67.23	-	19.79
	VideoDPO	79.80	83.00	66.99	-	19.79

Table 1. **VideoDPO alignment performance.** We apply our proposed VideoDPO on three state-of-the-art open-source models and evaluate performance on VBench, HPS (V), and PickScore. After training with VideoDPO, all models achieve the best performance on VBench, with improvements also observed on HPS (V) or PickScore, demonstrating the effectiveness of our approach.

5.2. Dataset Analysis

Score distribution and sub-dimension correlations. We analyze the dataset by examining the OmniScore distribution, the score range, *i.e.*, the difference between maximum and minimum scores, for each prompt, and the correlations among individual scoring metrics. To quantify these correlations, we calculate Pearson correlation coefficients. For each prompt, N videos are generated and assigned OmniScore, enabling us to assess the distribution of score differences, *i.e.*, the range between the highest and lowest scores, within each set of N videos. Fig. 3 presents both the overall score distribution and the distribution of score differences between video pairs.

5.3. Aligning Video Diffusion Models

In this section, we evaluate our approach through both quantitative and qualitative results by testing on various text-to-video models. For quantitative evaluation, we utilize VBench, HPS (V), and PickScore, covering both non-human and human preference metrics. To evaluate semantic alignment and visual quality, we analyze intra-frame aspects, examining image fidelity and aesthetic appeal to ensure each frame aligns well with the prompt. Additionally, for inter-frame analysis, we assess temporal consistency, focusing on whether the background and main foreground objects remain coherent across frames.

Quantitative results. We present our results in Tab. 1, where we evaluate state-of-the-art open-source text-to-video models, including VC2, T2VTurbo, and CogVideo. After alignment using our approach, all models show performance improvements, with consistent gains on the VBench metric. Models such as VC2 and T2VTurbo also achieve higher scores on human preference metrics, including HPS (V) and PickScore, demonstrating the generalizability of our approach. We do not report CogVideo on HPS (V) as this score appears to be insensitive to CogVideo, possibly due to the low quality generation, given its early release date. The detailed performance results on VBench are presented in Tab. 2. In comparison to other RLHF methods like VADAR, our approach yields superior results in both semantic and visual quality aspects. This improvement is attributed to our use of preference pairs derived from a more comprehensive feedback signal, both quality(intra-frame and inter-frame levels) and semantic criteria. However, methods like VADER can only optimize a single differentiable reward model, limiting improvements in other dimensions. Training with VADER on multiple reward models simultaneously will significantly increase the computational cost, making it difficult to scale.

Intra-frame qualitative analysis. Fig. 4 presents qualitative comparisons achieved using VideoDPO on baseline models. Videos generated after VideoDPO demonstrate enhanced visual details with fewer artifacts (as shown in the

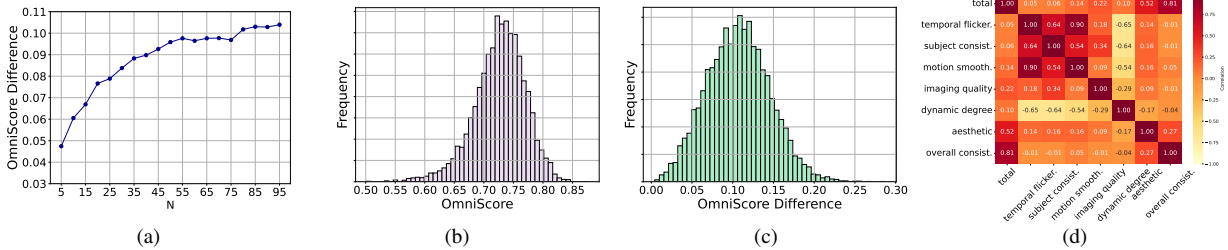


Figure 3. **Analysis of OmniScore.** (a) The difference between the maximum and minimum OmniScore among N videos as N increases. (b) Histogram of OmniScore. (c) Histogram of the difference in OmniScore between two samples in a preference pair. (d) Correlation heatmap of the OmniScore across dimensions.

	Model	Total	Motion smooth.	Dynamic degree	Aesthetic quality	Object class	Multiple objects	Human action	Spatial relation.	Scene	Appear. style	Subject consist.	Back. consist.
VC2	Baseline [7]	80.44	97.73	42.50	63.13	92.55	40.66	95.00	35.86	55.29	87.84	96.85	98.22
	VideoDPO	81.93	92.18	32.64	63.18	97.15	52.29	99.00	48.71	71.07	88.65	95.69	96.98
Turbo	Baseline [26]	80.95	87.27	27.78	68.57	93.20	51.83	96.00	40.98	62.67	85.07	96.12	97.62
	VideoDPO	81.80	88.85	29.86	68.98	93.59	51.98	94.00	37.68	65.23	86.05	96.10	97.68
CogV.	Baseline [19]	79.30	89.64	31.25	61.25	80.06	52.67	85.00	55.19	44.10	80.60	95.58	97.56
	VideoDPO	79.80	88.64	38.89	58.64	77.22	54.04	81.00	54.90	45.69	79.73	94.67	96.64

Table 2. **Comparison of sub-dimension scores before and after alignment** on VBench for VC2, T2VTurbo and CogVideo.

Quality column) and improved alignment with the input prompt (as shown in the Semantic column). For instance, Turbo-VideoDPO produces a more accurate vase compared to the original model, where the vase’s mouth is incorrectly shaped. Similarly, the video from CogVideo-VideoDPO is better than that by CogVideo which contains unnatural color artifacts in the dog. In terms of semantic accuracy, VC2-VideoDPO generates a boat with visible human figures, offering a more accurate depiction compared to both VC2-VADER and the original VC2. Additionally, Turbo and CogVideo after training with our method, each generates more realistic character relationships and scene layouts correspondingly. These improvements demonstrate that our alignment approach successfully enhances both semantic following and visual fidelity in generated videos.

Inter-frame qualitative analysis. Our approach significantly improves the temporal consistency of aligned models, and Fig. 5 shows the comparison results. After alignment, VC2 is able to generate a stable stop sign, Turbo produces a scene where the number of giraffes remains consistent, and CogVideo generates a panda with stable coloring, avoiding sudden color changes. These examples demonstrate the effectiveness of our alignment method in enhancing temporal stability across frames, in terms of texts, object and color across different frames.

5.4. Analysis

Comparing OmniScore with single-aspect reward. We compare the setting trained using OmniScore with those

trained using a single reward, such as only the semantic score or the aesthetic score. On VBench, the results are 80.20% and 79.65%, which are significantly lower than the result achieved with OmniScore, which is 81.93%. This demonstrates the advantage of using a comprehensive reward like OmniScore to evaluate samples. The comparison with VADER in Tab. 1, also supports this conclusion.

Pairwise training strategies. We explore different strategies for constructing preference pairs from N generated videos for a prompt, shown in Tab. 3a. The “Better-Worse” strategy outputs multiple pairs (v_i, v_j) as long as $s_i > s_j$, representing the score of video v_i is higher than that of v_j . The “Best-vs-Worse” strategy forms pairs by selecting the highest-scoring video and pairing it with others that have lower scores. In contrast, the “Better-vs-Worst” strategy pairs the lowest-scoring video with others. The “Best-vs-Worst” strategy, adopted by us, pairs only the highest and lowest-scoring videos and outputs 1 preference pair for a prompt. The experiments show that this strategy, which generates only the most distinctive pair, yields the best performance. This demonstrates that the key to the alignment performance lies in the average quality of the preference, rather than the absolute quantity of data.

Data filtering. According to Fig. 3, there are some preference pairs are not distinctive, that the positive video is only slightly better than the negative one in terms of the OmniScore. We explored the impact of removing these less-distinctive pairs to see if it could improve alignment perfor-

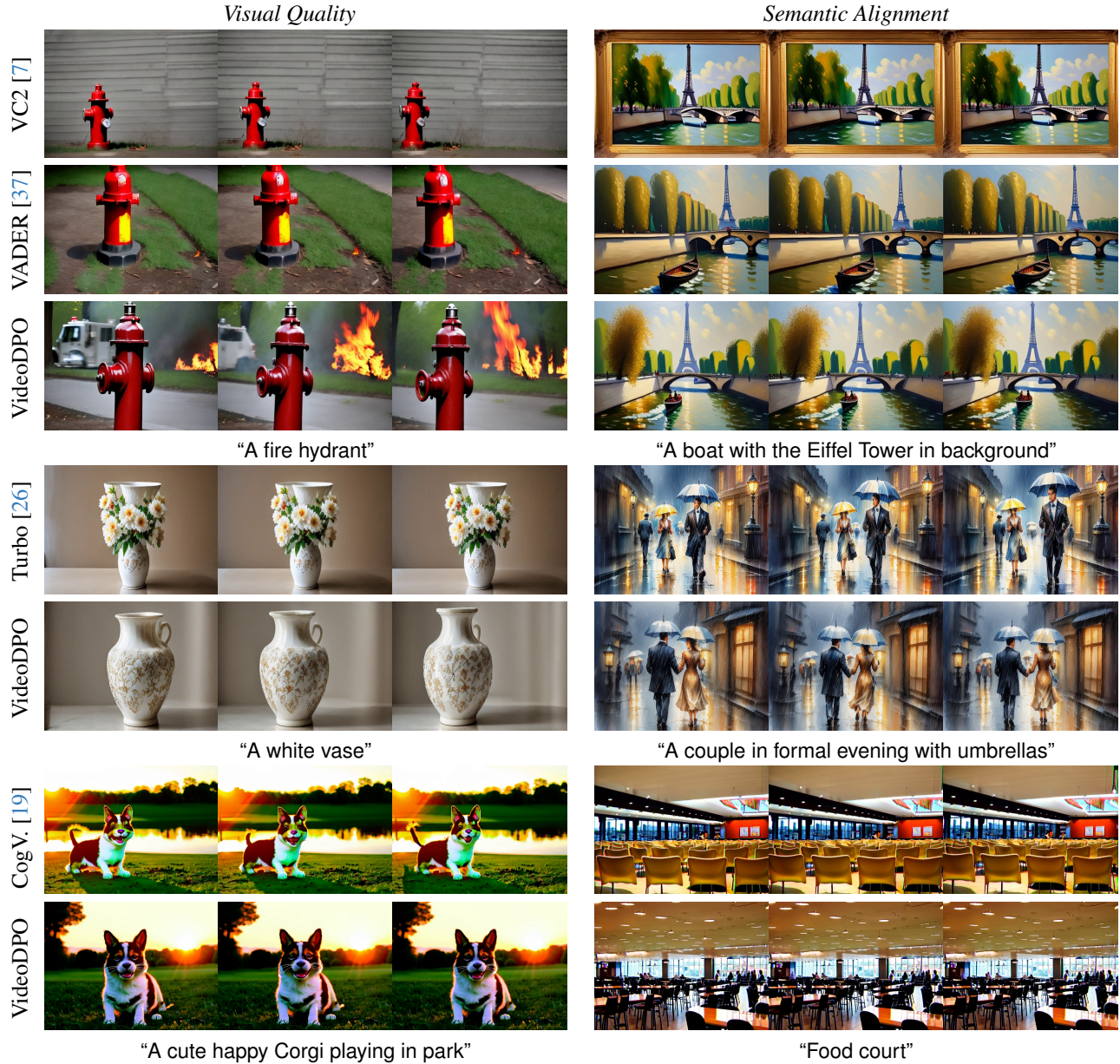


Figure 4. **Intra-frame qualitative visualization.** VideoDPO enables the model to generate videos with improved image quality and stronger semantic alignment. *Left:* Comparison of Image Quality. It avoids generating objects with strange colors and reduces visual artifacts (e.g., in the dog case), while producing harmonious objects (e.g., fire hydrants, vases). *Right:* Comparison of Semantic Alignment. It generates correct scenes (e.g., restaurant), accurate character relationships (e.g., couple), and proper visual elements (e.g., boat).

mance. However, the results in Tab. 3b show that excluding these training samples led to worse performance. This may be because the removal of these pairs, also including the prompts, reduced the diversity of the training data, leaving the model with many prompts it had not seen before and weakening its alignment performance. Though the pairs distinctiveness of these prompts are small, they still play a crucial role in the alignment.

Preference re-weighting scale. Determining the scale of re-weighting for distinctive preference pairs is impor-

tant. Here, we explore the impact of different values of α on alignment learning performance. When $\alpha = 0$, all pairs are assigned equal weight, disabling the re-weighting mechanism as a vanilla DPO. A higher α value increases the weight assigned to rare preference pairs. As shown in Tab. 3c, a value of $\alpha = 1$ performs significantly better than $\alpha = 0.5$, providing a reference for the model’s weight scaling. At $\alpha = 2$, we observe a significant increase in semantic performance but a decrease in quality performance on VBench, resulting in the same total score as achieved with

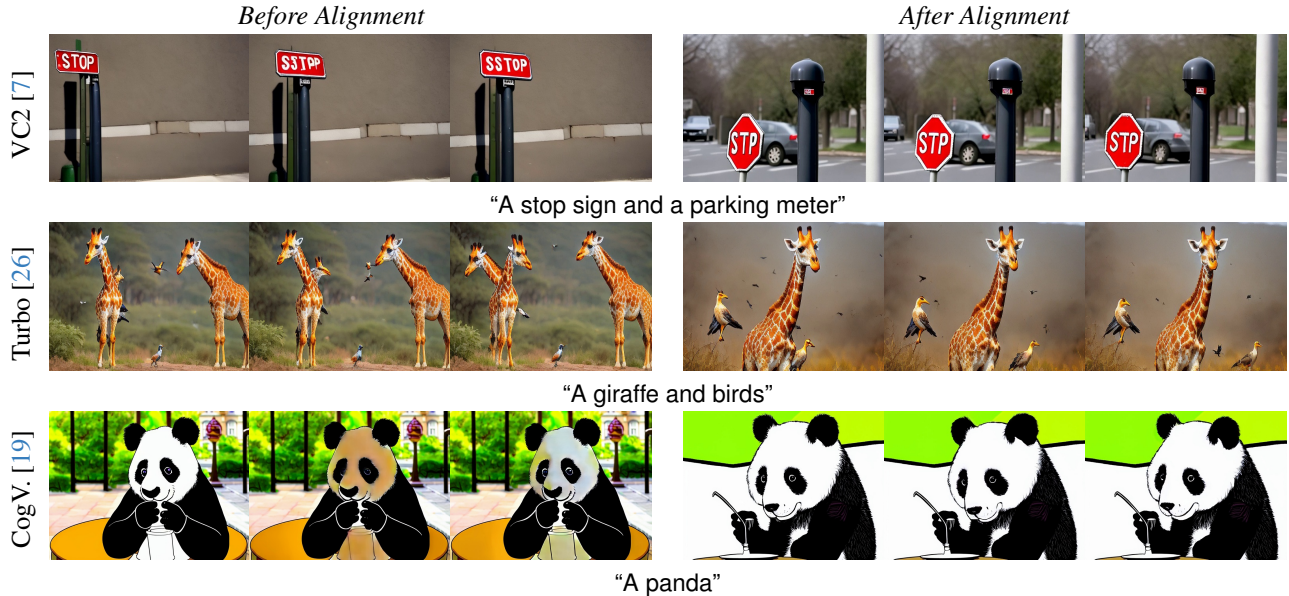


Figure 5. **Inter-frame qualitative visualization.** VideoDPO improves inter-frame consistency quality. The aligned model generates stable text like in the signboard, maintains consistent object appearances such as the giraffe, and ensures uniform color tones, as seen with pandas.

Method	VBench (%)			HPS (V)	PickScore
	Total	Q	S		
better vs. worse	81.32	83.46	72.74	0.258	20.62
best vs. worse	80.80	82.74	73.03	0.258	20.62
better vs. worst	80.73	82.40	74.08	0.259	20.67
best vs. worst	81.93	83.07	77.38	0.261	20.65

(a) Performance on different pairing strategies.

α	VBench (%)			HPS (V)	PickScore
	Total	Q	S		
0.0 <i>Vanilla DPO</i>	80.89	82.78	73.32	0.260	20.64
0.5	81.51	82.99	75.60	0.260	20.68
1.0 <i>Ours</i>	81.93	83.07	77.38	0.261	20.65
2.0	81.93	82.52	79.59	0.260	20.70

(c) Different values of α .

Method	VBench (%)			HPS (V)	PickScore
	Total	Q	S		
-75	80.08	81.53	74.29	0.259	20.64
-50	81.29	82.94	74.68	0.259	20.57
-25	81.42	83.16	74.49	0.258	20.65
Full	81.93	83.07	77.38	0.261	20.65

(b) Filtering out the least distinct pairs at different ratios.

N	VBench (%)			HPS (V)	PickScore
	Total	Q	S		
2	80.89	82.78	73.32	0.260	20.60
3	81.51	82.99	75.60	0.260	20.62
4	81.93	83.07	77.38	0.261	20.65

(d) Different values of N .

Table 3. **Ablation studies.** We study different strategies and configurations including (a) the pair strategy, (b) the filter strategy, (c) α values, the tuning hyper-parameter for re-weighting, and (d) N values, the number of video samples for each text prompt. **Q** is short for visual quality and **S** is short for semantic alignment.

$\alpha = 1$. All non-zero values of α improve performance, demonstrating the robustness of the re-weighting approach.

Comparing with supervised fine-tuning. We compare VideoDPO with supervised fine-tuning (SFT), a baseline approach of post-training for pre-trained models. In SFT, only winning samples v^W are used to fine-tune the model, while all other settings remain the same. Tab. 1 shows for models like VC2 and CogVideo, VideoDPO shows a clear advantage over SFT. This suggests the importance of learning from negative samples, which reduces the likelihood of generating lower-quality outputs.

Effect of varying N on performance. We investigate the impact of generating different numbers of videos N on model performance. As shown in Fig. 3, a larger N tends to produce more distinctive samples. Tab. 3d presents the experimental results for varying values of N , indicating that performance improves as N increases. However, a larger N also increases the cost of dataset generation. Determining the optimal balance between performance gain and data generation cost as N grows remains an open question.

6. Conclusion

In this paper, we propose VideoDPO, a novel pipeline to align video diffusion models. VideoDPO introduces

a comprehensive scoring method, OmniScore, along with a novel data reweighting strategy that automatically constructs and prioritizes preference data, enabling more effective alignment training. Experiments show that VideoDPO enhances both visual quality and semantic alignment for state-of-the-art text-to-video models.

References

- [1] Gen-2. Accessed September 25, 2023 [Online] <https://research.runwayml.com/gen2>, 2023. 2
- [2] Andreas Blattmann, Tim Dockhorn, Sumith Kulal, Daniel Mendelevitch, Maciej Kilian, Dominik Lorenz, Yam Levi, Zion English, Vikram Voleti, Adam Letts, et al. Stable video diffusion: Scaling latent video diffusion models to large datasets. *arXiv preprint arXiv:2311.15127*, 2023. 2
- [3] Emanuele Bugliarello, Hernan Moraldo, Ruben Villegas, Mohammad Babaeizadeh, Mohammad Taghi Saffar, Han Zhang, Dumitru Erhan, Vittorio Ferrari, Pieter-Jan Kindermans, and Paul Voigtlaender. StoryBench: A Multifaceted Benchmark for Continuous Story Visualization. In *Advances in Neural Information Processing Systems*. Curran Associates, Inc., 2023. 3
- [4] Mathilde Caron, Hugo Touvron, Ishan Misra, Hervé Jégou, Julien Mairal, Piotr Bojanowski, and Armand Joulin. Emerging properties in self-supervised vision transformers. In *ICCV*, 2021. 1
- [5] Haoxuan Che, Xuanhua He, Quande Liu, Cheng Jin, and Hao Chen. Gamegen-x: Interactive open-world game video generation. *arXiv preprint arXiv:2411.00769*, 2024. 2
- [6] Haoxin Chen, Menghan Xia, Yingqing He, Yong Zhang, Xiaodong Cun, Shaoshu Yang, Jinbo Xing, Yaofang Liu, Qifeng Chen, Xintao Wang, Chao Weng, and Ying Shan. Videocrafter1: Open diffusion models for high-quality video generation, 2023. 2
- [7] Haoxin Chen, Yong Zhang, Xiaodong Cun, Menghan Xia, Xintao Wang, Chao Weng, and Ying Shan. Videocrafter2: Overcoming data limitations for high-quality video diffusion models, 2024. 2, 5, 6, 7, 8, 3
- [8] Junsong Chen, Jincheng Yu, Chongjian Ge, Lewei Yao, Enze Xie, Yue Wu, Zhongdao Wang, James Kwok, Ping Luo, Huchuan Lu, and Zhenguo Li. Pixart- α : Fast training of diffusion transformer for photorealistic text-to-image synthesis, 2023. 2
- [9] Xiaoyu Chen, Junliang Guo, Tianyu He, Chuheng Zhang, Pushi Zhang, Derek Cathera Yang, Li Zhao, and Jiang Bian. Igor: Image-goal representations are the atomic control units for foundation models in embodied ai. *arXiv preprint arXiv:2411.00785*, 2024. 2
- [10] Xiaoliang Dai, Ji Hou, Chih-Yao Ma, Sam Tsai, Jialiang Wang, Rui Wang, Peizhao Zhang, Simon Vandenhende, Xiao-fang Wang, Abhimanyu Dubey, et al. Emu: Enhancing image generation models using photogenic needles in a haystack. *arXiv preprint arXiv:2309.15807*, 2023. 2
- [11] Yuming Fang, Hanwei Zhu, Yan Zeng, Kede Ma, and Zhou Wang. Perceptual quality assessment of smartphone photography. In *CVPR*, 2020. 1
- [12] Lanqing Guo, Yingqing He, Haoxin Chen, Menghan Xia, Xiaodong Cun, Yufei Wang, Siyu Huang, Yong Zhang, Xintao Wang, Qifeng Chen, et al. Make a cheap scaling: A self-cascade diffusion model for higher-resolution adaptation. In *European Conference on Computer Vision*, pages 39–55. Springer, 2025. 2
- [13] Jingwen He, Tianfan Xue, Dongyang Liu, Xinqi Lin, Peng Gao, Dahua Lin, Yu Qiao, Wanli Ouyang, and Ziwei Liu. Venhancer: Generative space-time enhancement for video generation. *arXiv preprint arXiv:2407.07667*, 2024. 2
- [14] Yingqing He, Tianyu Yang, Yong Zhang, Ying Shan, and Qifeng Chen. Latent video diffusion models for high-fidelity long video generation. 2022. 2
- [15] Yingqing He, Menghan Xia, Haoxin Chen, Xiaodong Cun, Yuan Gong, Jinbo Xing, Yong Zhang, Xintao Wang, Chao Weng, Ying Shan, et al. Animate-a-story: Storytelling with retrieval-augmented video generation. *arXiv preprint arXiv:2307.06940*, 2023. 2
- [16] Yingqing He, Shaoshu Yang, Haoxin Chen, Xiaodong Cun, Menghan Xia, Yong Zhang, Xintao Wang, Ran He, Qifeng Chen, and Ying Shan. Scalecrafter: Tuning-free higher-resolution visual generation with diffusion models. In *The Twelfth International Conference on Learning Representations*, 2023. 2
- [17] Martin Heusel, Hubert Ramsauer, Thomas Unterthiner, Bernhard Nessler, and Sepp Hochreiter. GANs trained by a two time-scale update rule converge to a local nash equilibrium. In *NeurIPS*, 2017. 2
- [18] Jonathan Ho, Ajay Jain, and Pieter Abbeel. Denoising diffusion probabilistic models. *CoRR*, abs/2006.11239, 2020. 2
- [19] Wenyi Hong, Ming Ding, Wendi Zheng, Xinghan Liu, and Jie Tang. Cogvideo: Large-scale pretraining for text-to-video generation via transformers. *arXiv preprint arXiv:2205.15868*, 2022. 2, 5, 6, 7, 8, 3
- [20] Kaiyi Huang, Kaiyue Sun, Enze Xie, Zhenguo Li, and Xihui Liu. T2i-compbench: A comprehensive benchmark for open-world compositional text-to-image generation. *arXiv preprint arXiv: 2307.06350*, 2023. 2
- [21] Ziqi Huang, Yanan He, Jiashuo Yu, Fan Zhang, Chenyang Si, Yuming Jiang, Yuanhan Zhang, Tianxing Wu, Qingyang Jin, Nattapol Chanpaisit, Yaohui Wang, Xinyuan Chen, Limin Wang, Dahua Lin, Yu Qiao, and Ziwei Liu. VBench: Comprehensive benchmark suite for video generative models. In *Proceedings of the IEEE/CVF Conference on Computer Vision and Pattern Recognition*, 2024. 3, 1
- [22] Junjie Ke, Qifei Wang, Yilin Wang, Peyman Milanfar, and Feng Yang. MUSIC: multi-scale image quality transformer. *CoRR*, abs/2108.05997, 2021. 3, 1
- [23] Yuval Kirstain, Adam Polyak, Uriel Singer, Shahbuland Matiana, Joe Penna, and Omer Levy. Pick-a-pic: An open dataset of user preferences for text-to-image generation. *Advances in Neural Information Processing Systems*, 36: 36652–36663, 2023. 1, 5
- [24] LAION-AI. aesthetic-predictor. <https://github.com/LAION-AI/aesthetic-predictor>, 2022. 1
- [25] Tony Lee, Michihiro Yasunaga, Chenlin Meng, Yifan Mai, Joon Sung Park, Agrim Gupta, Yunzhi Zhang, Deepak

- Narayanan, Hannah Benita Teufel, Marco Bellagente, et al. Holistic evaluation of text-to-image models. *arXiv preprint arXiv:2311.04287*, 2023. 2
- [26] Jiachen Li, Weixi Feng, Tsu-Jui Fu, Xinyi Wang, Sugato Basu, Wenhui Chen, and William Yang Wang. T2v-turbo: Breaking the quality bottleneck of video consistency model with mixed reward feedback. In *Advances in neural information processing systems*, 2024. 2, 5, 6, 7, 8, 3
- [27] Jiachen Li, Long Qian, Jian Zheng, Xiaofeng Gao, Robinson Piramuthu, Wenhui Chen, and William Yang Wang. T2v-turbo-v2: Enhancing video generation model post-training through data, reward, and conditional guidance design, 2024. 2
- [28] Zhen Li, Zuo-Liang Zhu, Ling-Hao Han, Qibin Hou, Chun-Le Guo, and Ming-Ming Cheng. Amt: All-pairs multi-field transforms for efficient frame interpolation. In *CVPR*, 2023. 1
- [29] Zhanhao Liang, Yuhui Yuan, Shuyang Gu, Bohan Chen, Tiankai Hang, Ji Li, and Liang Zheng. Step-aware preference optimization: Aligning preference with denoising performance at each step. *arXiv preprint arXiv:2406.04314*, 2024. 2
- [30] Mingxiang Liao, Hannan Lu, Xinyu Zhang, Fang Wan, Tianyu Wang, Yuzhong Zhao, Wangmeng Zuo, Qixiang Ye, and Jingdong Wang. Evaluation of text-to-video generation models: A dynamics perspective. *arXiv preprint arXiv:2407.01094*, 2024. 3
- [31] Jiahe Liu, Youran Qu, Qi Yan, Xiaohui Zeng, Lele Wang, and Renjie Liao. Fr\`echet video motion distance: A metric for evaluating motion consistency in videos. *arXiv preprint arXiv:2407.16124*, 2024. 3
- [32] Yaofang Liu, Xiaodong Cun, Xuebo Liu, Xintao Wang, Yong Zhang, Haoxin Chen, Yang Liu, Tiejong Zeng, Raymond Chan, and Ying Shan. Evalcrafter: Benchmarking and evaluating large video generation models. *arXiv preprint arXiv:2310.11440*, 2023. 3
- [33] Yuanxin Liu, Lei Li, Shuhuai Ren, Rundong Gao, Shicheng Li, Sishuo Chen, Xu Sun, and Lu Hou. Fetv: A benchmark for fine-grained evaluation of open-domain text-to-video generation. In *NeurIPS*, 2023. 3
- [34] Yue Ma, Yingqing He, Xiaodong Cun, Xintao Wang, Siran Chen, Xiu Li, and Qifeng Chen. Follow your pose: Pose-guided text-to-video generation using pose-free videos. In *Proceedings of the AAAI Conference on Artificial Intelligence*, pages 4117–4125, 2024. 2
- [35] Yue Ma, Yingqing He, Hongfa Wang, Andong Wang, Chenyang Qi, Chengfei Cai, Xiu Li, Zhifeng Li, Heung-Yeung Shum, Wei Liu, et al. Follow-your-click: Open-domain regional image animation via short prompts. *arXiv preprint arXiv:2403.08268*, 2024. 2
- [36] William Peebles and Saining Xie. Scalable diffusion models with transformers. *arXiv preprint arXiv:2212.09748*, 2022. 2
- [37] Mihir Prabhudesai, Russell Mendonca, Zheyang Qin, Katerina Fragkiadaki, and Deepak Pathak. Video diffusion alignment via reward gradients, 2024. 2, 5, 7, 3
- [38] Alec Radford, Jong Wook Kim, Chris Hallacy, Aditya Ramesh, Gabriel Goh, Sandhini Agarwal, Girish Sastry, Amanda Askell, Pamela Mishkin, Jack Clark, et al. Learning transferable visual models from natural language supervision. In *ICML*, 2021. 2, 3
- [39] Rafael Rafailov, Archit Sharma, Eric Mitchell, Christopher D Manning, Stefano Ermon, and Chelsea Finn. Direct preference optimization: Your language model is secretly a reward model. In *Thirty-seventh Conference on Neural Information Processing Systems*, 2023. 1, 2, 3
- [40] Chitwan Saharia, William Chan, Saurabh Saxena, Lala Li, Jay Whang, Emily Denton, Seyed Kamyar Seyed Ghasemipour, Burcu Karagol Ayan, S Sara Mahdavi, Rapha Gontijo Lopes, et al. Photorealistic text-to-image diffusion models with deep language understanding. *arXiv preprint arXiv:2205.11487*, 2022. 3
- [41] Tim Salimans, Ian Goodfellow, Wojciech Zaremba, Vicki Cheung, Alec Radford, Xi Chen, and Xi Chen. Improved techniques for training gans. In *NeurIPS*, 2016. 2
- [42] C Schuhmann. Laoin aesthetic predictor. 2022. 3
- [43] John Schulman, Filip Wolski, Prafulla Dhariwal, Alec Radford, and Oleg Klimov. Proximal policy optimization algorithms. *arXiv preprint arXiv:1707.06347*, 2017. 2
- [44] Jascha Sohl-Dickstein, Eric A. Weiss, Niru Maheswaranathan, and Surya Ganguli. Deep unsupervised learning using nonequilibrium thermodynamics, 2015. 2
- [45] Kaiyue Sun, Kaiyi Huang, Xian Liu, Yue Wu, Zihan Xu, Zhenguo Li, and Xihui Liu. T2v-compbench: A comprehensive benchmark for compositional text-to-video generation. *arXiv preprint arXiv:2407.14505*, 2024. 3
- [46] Zachary Teed and Jia Deng. Raft: Recurrent all-pairs field transforms for optical flow. In *ECCV*, 2020. 3, 1
- [47] Thomas Unterthiner, Sjoerd van Steenkiste, Karol Kurach, Raphael Marinier, Marcin Michalski, and Sylvain Gelly. Towards accurate generative models of video: A new metric & challenges. *arXiv preprint arXiv:1812.01717*, 2018. 2
- [48] Bram Wallace, Meihua Dang, Rafael Rafailov, Linqi Zhou, Aaron Lou, Senthil Purushwalkam, Stefano Ermon, Caiming Xiong, Shafiq Joty, and Nikhil Naik. Diffusion model alignment using direct preference optimization, 2023. 1, 2, 3
- [49] Jiuniu Wang, Hangjie Yuan, Dayou Chen, Yingya Zhang, Xiang Wang, and Shiwei Zhang. Modelscope text-to-video technical report. *arXiv preprint arXiv:2308.06571*, 2023. 2
- [50] Su Wang, Chitwan Saharia, Ceslee Montgomery, Jordi Pont-Tuset, Shai Noy, Stefano Pellegrini, Yasumasa Onoe, Sarah Laszlo, David J Fleet, Radu Soricut, et al. Imagen editor and EditBench: Advancing and evaluating text-guided image inpainting. *arXiv preprint arXiv:2212.06909*, 2022. 3
- [51] Wenhao Wang and Yi Yang. Vidprom: A million-scale real prompt-gallery dataset for text-to-video diffusion models. *arXiv preprint arXiv:2403.06098*, 2024. 4, 5
- [52] Xinlong Wang, Xiaosong Zhang, Zhengxiong Luo, Quan Sun, Yufeng Cui, Jinsheng Wang, Fan Zhang, Yueze Wang, Zhen Li, Qiyang Yu, et al. Emu3: Next-token prediction is all you need. *arXiv preprint arXiv:2409.18869*, 2024. 2
- [53] Yi Wang, Yanan He, Yizhuo Li, Kunchang Li, Jiashuo Yu, Xin Ma, Xinyuan Chen, Yaohui Wang, Ping Luo, Ziwei Liu, Yali Wang, Limin Wang, and Yu Qiao. Internvid: A large-scale video-text dataset for multimodal understanding and generation. *arXiv preprint arXiv:2307.06942*, 2023. 1

- [54] Wenming Weng, Ruoyu Feng, Yanhui Wang, Qi Dai, Chunyu Wang, Dacheng Yin, Zhiyuan Zhao, Kai Qiu, Jianmin Bao, Yuhui Yuan, Chong Luo, Yueyi Zhang, and Zhiwei Xiong. Art•v: Auto-regressive text-to-video generation with diffusion models. *arXiv preprint arXiv:2311.18834*, 2023. [2](#)
- [55] Jay Zhangjie Wu, Guian Fang, Haoning Wu, Xintao Wang, Yixiao Ge, Xiaodong Cun, David Junhao Zhang, Jia-Wei Liu, Yuchao Gu, Rui Zhao, Weisi Lin, Wynne Hsu, Ying Shan, and Mike Zheng Shou. Towards a better metric for text-to-video generation. *arXiv preprint arXiv:2401.07781*, 2024. [3](#)
- [56] Xiaoshi Wu, Yiming Hao, Keqiang Sun, Yixiong Chen, Feng Zhu, Rui Zhao, and Hongsheng Li. Human preference score v2: A solid benchmark for evaluating human preferences of text-to-image synthesis. *arXiv preprint arXiv:2306.09341*, 2023. [5](#)
- [57] Haoran Xu, Amr Sharaf, Yunmo Chen, Weiting Tan, Lingfeng Shen, Benjamin Van Durme, Kenton Murray, and Young Jin Kim. Contrastive preference optimization: Pushing the boundaries of LLM performance in machine translation. *ArXiv*, abs/2401.08417, 2024. [2](#)
- [58] Zhuoyi Yang, Jiayan Teng, Wendi Zheng, Ming Ding, Shiyu Huang, Jiazheng Xu, Yuanming Yang, Wenyi Hong, Xiaohan Zhang, Guanyu Feng, et al. Cogvideox: Text-to-video diffusion models with an expert transformer. *arXiv preprint arXiv:2408.06072*, 2024. [2](#)
- [59] Hongyi Yuan, Zheng Yuan, Chuanqi Tan, Wei Wang, Songfang Huang, and Fei Huang. RRHF: Rank responses to align language models with human feedback. In *NeurIPS*, 2023. [2](#)
- [60] Hangjie Yuan, Shiwei Zhang, Xiang Wang, Yujie Wei, Tao Feng, Yining Pan, Yingya Zhang, Ziwei Liu, Samuel Albanie, and Dong Ni. Instructvideo: Instructing video diffusion models with human feedback. 2023. [2](#)
- [61] Shenghai Yuan, Jinfa Huang, Yongqi Xu, Yaoyang Liu, Shaofeng Zhang, Yujun Shi, Ruijie Zhu, Xinhua Cheng, Jiebo Luo, and Li Yuan. Chronomagic-bench: A benchmark for metamorphic evaluation of text-to-time-lapse video generation. *arXiv preprint arXiv:2406.18522*, 2024. [3](#)
- [62] Yao Zhao, Rishabh Joshi, Tianqi Liu, Misha Khalman, Mohammad Saleh, and Peter J. Liu. SLiC-HF: Sequence likelihood calibration with human feedback. *ArXiv*, abs/2305.10425, 2023. [2](#)
- [63] Zangwei Zheng, Xiangyu Peng, Tianji Yang, Chenhui Shen, Shenggui Li, Hongxin Liu, Yukun Zhou, Tianyi Li, and Yang You. Open-sora: Democratizing efficient video production for all, 2024. [2](#)

VideoDPO: Omni-Preference Alignment for Video Diffusion Generation

Supplementary Material

This supplementary material presents OmniScore details, additional analysis and experimental results. Section A enumerates the details of OmniScore, including the model each dimension utilizes and the corresponding weights. Section B compares the performance of single-dimensional, multi-dimensional settings and aggregation methods, also examines the impact of training data scale on the results. Section C includes additional intra-frame and inter-frame qualitative results.

A. OmniScore Implementation.

Inspired by the models used in [21], we build OmniScore by referencing these models and their corresponding weights to evaluate the quality of video samples. [21] aims to evaluate the quality of video generative models, whereas our OmniScore targets assessing the quality of video samples specifically for preference learning. Here we demonstrate the detailed composition of OmniScore:

Motion Smoothness. We utilize the motion priors in the video frame interpolation model [28] to evaluate the smoothness of generated motions

Temporal Flickering. We take static frames by RAFT [46] and compute the mean absolute difference across frames.

Subject Consistency - For a subject (e.g., a person, a car, or a cat) in the video, we assess whether its appearance remains consistent throughout the whole video. To this end, we calculate the DINO [4] feature similarity across frames.

Imaging Quality . Imaging quality refers to the distortion (e.g., over-exposure, noise, blur) presented in the generated frames, and we evaluate it using the MUSIQ [22] image quality predictor trained on the SPAQ [11] dataset.

Aesthetic Quality . We evaluate the artistic and beauty value perceived by humans towards each video frame using the LAION aesthetic predictor [24].

Dynamic Degree We use RAFT [46] to estimate the degree of dynamics in synthesized videos.

Text-Video semantic alignment. We use overall video-text consistency computed by ViCLIP [53].

The following dimensions are scaled to the range [0, 1] based on the following values:

- **Subject Consistency:** Min = 0.1462, Max = 1.0
- **Temporal Flickering:** Min = 0.6293, Max = 1.0
- **Motion Smoothness:** Min = 0.706, Max = 0.9975
- **Overall Consistency:** Min = 0.0, Max = 0.364

The weights assigned to Motion Smoothness, Temporal Flickering, Subject Consistency, Imaging Quality, Aesthetic Quality and Dynamic Degree are all 4, and the weight for Text-Video Semantic Alignment is set to 1.

B. Additional Analysis

Single- vs. multi-dimensional score comparison. In Table 5, we explore the results of training on a single-dimensional reward score compared to training on our OmniScore. The experimental results show that OmniScore achieves the best performance, highlighting the importance of a comprehensive score for our framework.

Multi-dimensional score aggregation. We explore two methods for multi-dimensional score aggregation: (1) selecting 10,000 pairs based on our OmniScore and (2) Combine preference pairs from individual dimensions into a larger dataset so that the VC2 model is trained on 40,000 pairs, with 10,000 pairs selected from each of the four dimensions: semantics, aesthetics, motion smoothness, and dynamic degree. The results indicate that the second approach significantly lowers performance to 78.26% on VBench-Total, showing that using our OmniScore can achieve better performance.

Effect of training scale on performance. We compared the performance shown in Table 4 when using only half and 25% of the prompt data for training, observing a significant drop across all metrics. This result demonstrates that increasing the amount of prompt data in training yields substantially better performance. We attribute this to improved generalization, as the model aligns with a broader range of prompts. These experiments suggest that our method still has room for improvement, particularly with regard to the amount of data.

Data	VBench(%)			HPS (V)	PickScore
	Total	Quality	Semantic		
25%	80.21	81.70	74.26	0.259	20.66
50%	80.83	82.37	74.68	0.260	20.59
Full(ours)	81.93	83.07	77.38	0.261	20.65

Table 4. Scores for Different Dataset Sizes

C. Additional Qualitative Results

We present the results of inter-frame and intra-frame alignment before and after learning in Figure 6 and Figure 7, respectively, following the format of the main paper. The results demonstrate that our alignment method is effective across a wide range of prompts, improving temporal consistency, visual quality, and semantics.

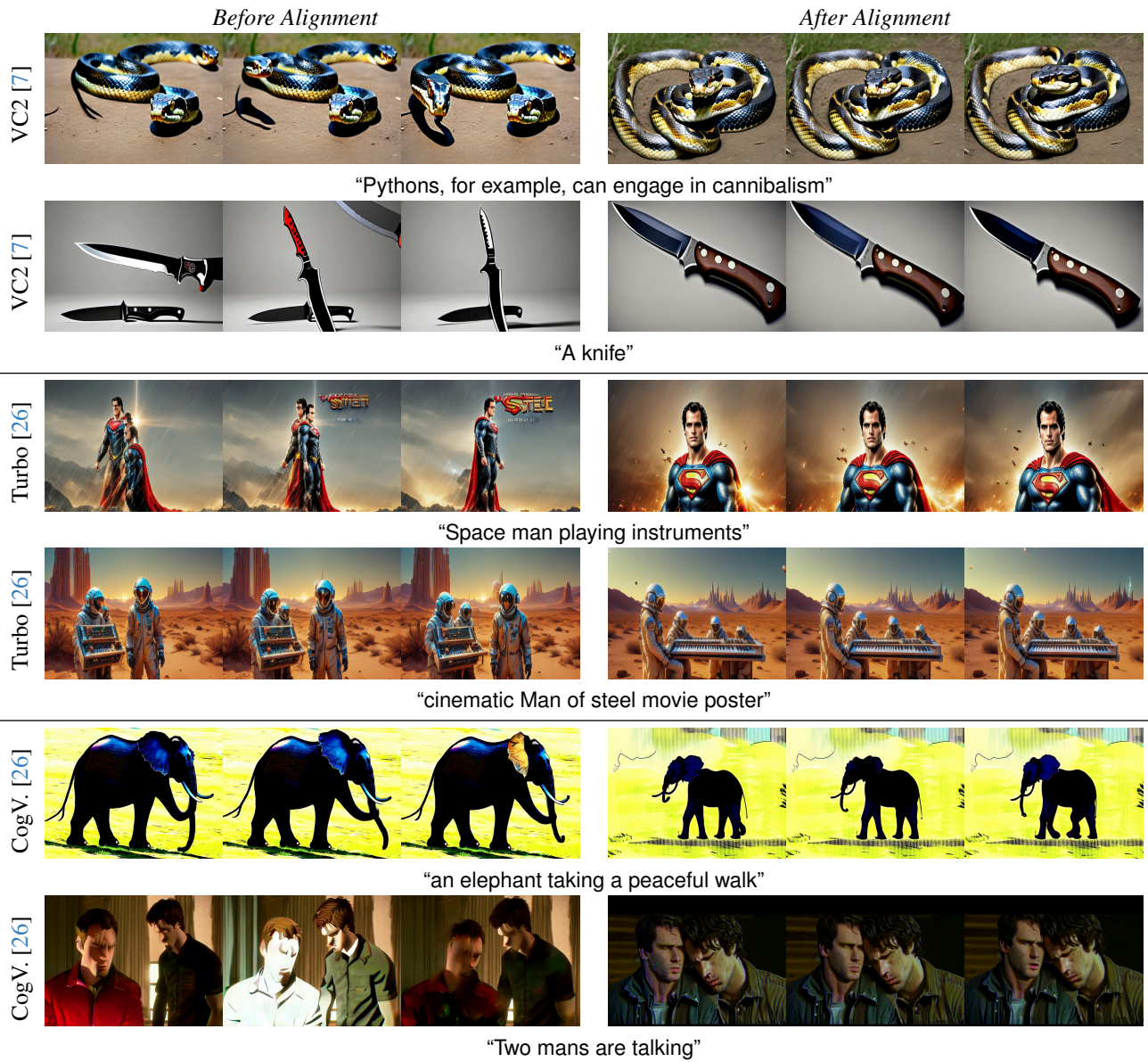


Figure 6. Additional inter-frame qualitative visualization.

Score	VBench (%)			Subject Consis.	Aesthetic Quality	Overall Consis.
	Total	Quality	Semantic			
Overall Consis.	80.20	81.57	74.74	95.61	62.94	78.76
Aesthetic Quality	79.65	81.67	71.57	97.13	63.27	76.98
Subject Consis.	77.05	79.00	69.28	94.25	58.23	73.35
OmniScore (ours)	81.93	83.07	77.38	95.69	63.18	78.43

Table 5. Scores for different training objectives include single-dimensional scores such as overall consistency, aesthetic quality, and subject consistency, as well as our multi-dimensional score, OmniScore. "Consis." is the abbreviation for "consistency."

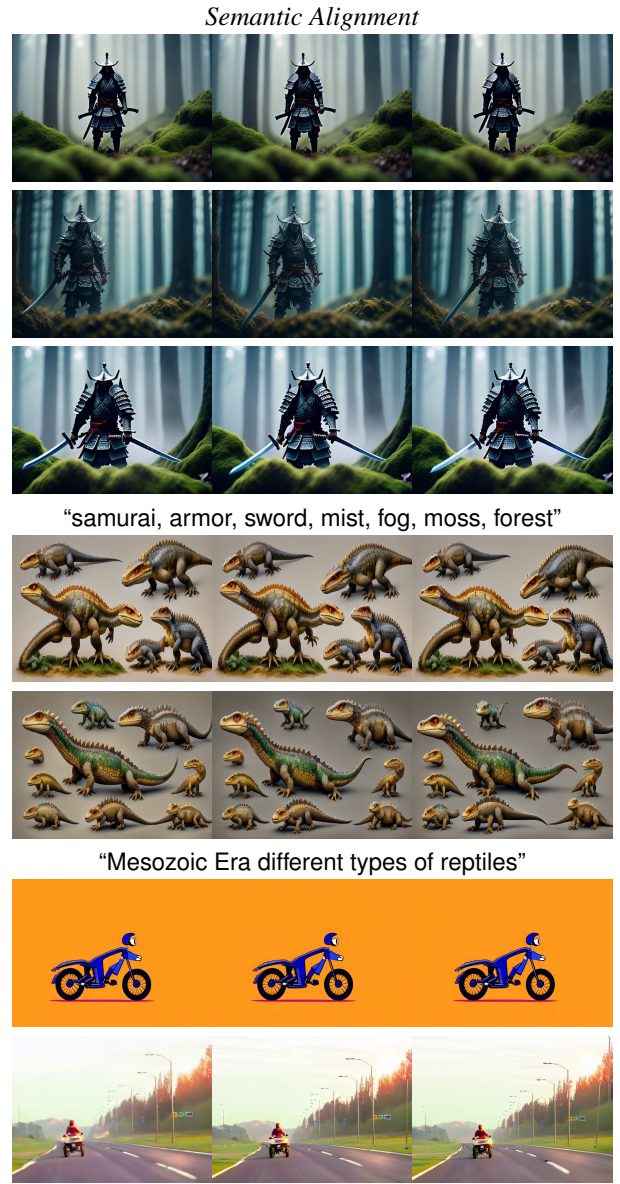
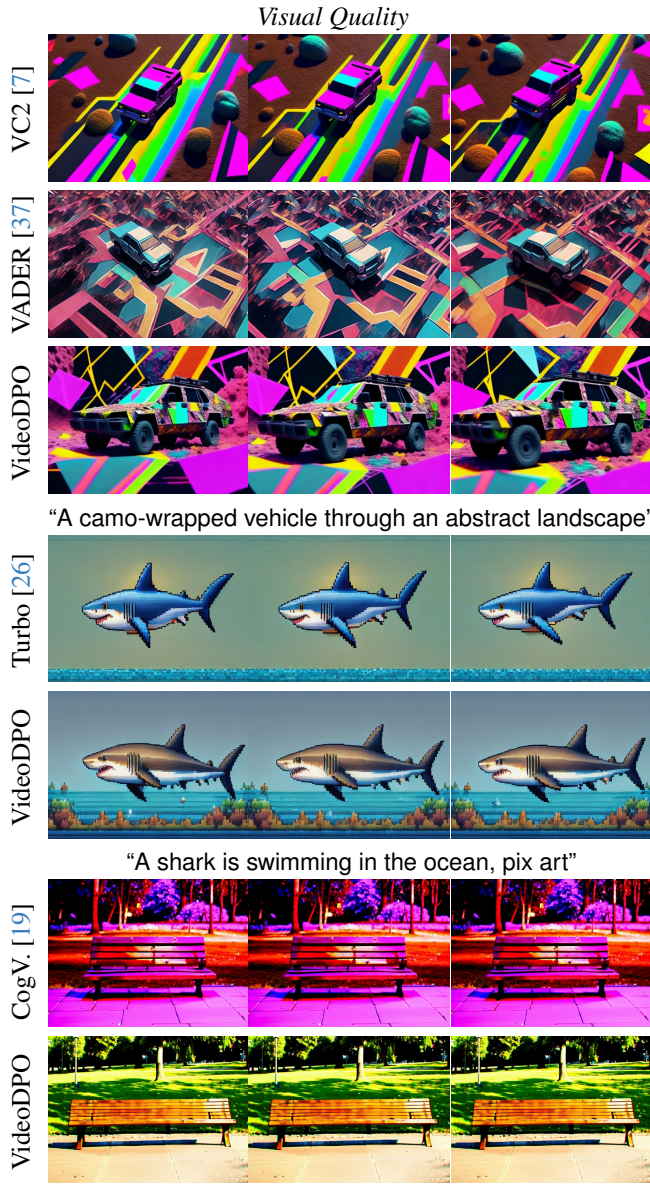


Figure 7. Additional intra-frame qualitative visualization.